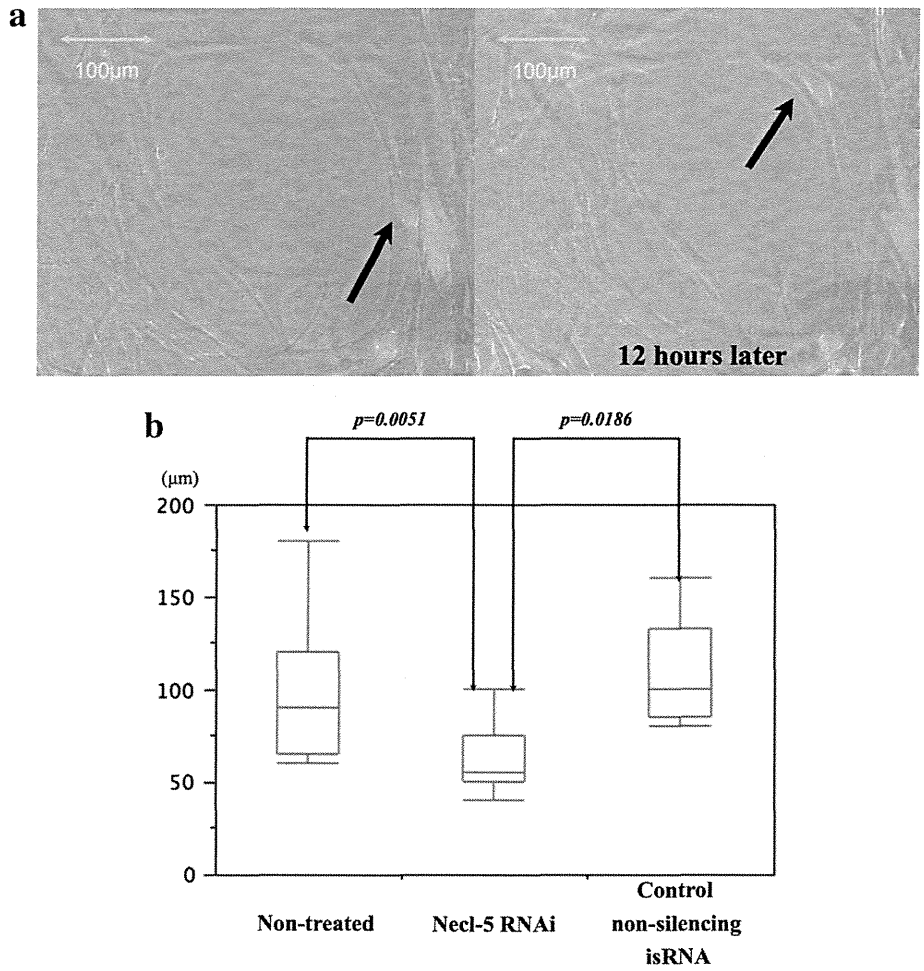

Fig. 6. *Comparison of Necl-5-transfected A549 cell movement.* (a) Neutral and fluorescent images (×100) of GFP-labeled A549s captured separately and then merged. From 48 h after the initiation of culture to 60 h, the distance of GFP-labeled A549 cells (marked with yellow arrows), which moved approximately 100 μm along the surface of fibroblasts, was calculated. (b) The group of A549 transfected with Necl-5 RNAi moved significantly slower compared to the non-treated group ($p=0.0051$) and the group transfected with control non-silencing ($p=0.0186$) ($n=10$ samples for each group).

that the cell shape does change during amoeba-like movement involving the cytoskeleton might reflect the EMT.

In this study, compared to fibroblasts, the BAC cells showed a strong expression of Necl-5. The tendency did not change even if the BAC cells were mixed with fibroblasts. The DL-CGH method also revealed that the inhibition of Necl-5 in tumor cells suppressed cell migration. This finding indicates that the expression of Necl-5 that originated in cancer cells might be crucial for the cancer–stromal communication, eventually leading to EMT. Therefore, Necl-5 could be a suitable molecular target for the suppression of cancer invasion in future studies.

We have previously shown the utility of DL-CGH, which enabled precise visualization of the invasive activity of cells precisely (Takata et al., 2007). Using this method, it would be feasible to conduct other large-scale RNAi experiments to screen for molecular gene targets against cancer infiltration. In contrast, it is difficult to assess cell proliferation by using this method. With regard to cell proliferation, we evaluated A549 cells only in cell culture dishes, and did not assess proliferation in the relation to fibroblasts. Further studies should be performed before the proliferative effects of Necl-5 on cancer–stromal interactions can be fully understood.

In conclusion, the expression of Necl-5 in tumor cells is associated with cell movement and proliferation. Furthermore, the DL-CGH method revealed that the knockdown of Necl-5 inhibited cancer invasiveness in cancer–stromal interactions. Necl-5 expression in tumor cells may play a crucial role in cancer–stromal communication and may be a potential molecular target for lung adenocarcinoma.

Conflict of interest statement

The authors declare that there are no conflicts of interest.

Appendix A. Supplementary data

Supplementary data to this article can be found online at http://dx.doi.org/10.1016/j.yexmp.2012.12.003.

References

Bellovin, D.I., Bates, R.C., Muzikansky, A., Rimm, D.L., Mercurio, A.M., 2005. Altered localization of p120 catenin during epithelial to mesenchymal transition of colon carcinoma is prognostic for aggressive disease. Cancer Research 65, 10938–10945.

Chadeneau, C., LeMoullac, B., Denis, M.G., 1994. A novel member of the immunoglobulin gene superfamily expressed in rat carcinoma cell lines. The Journal of Biological Chemistry 269, 15601–15605.

Doi, T., Maniwa, Y., Tanaka, Y., Tane, S., Hashimoto, S., Ohno, Y., Nishio, W., Nishimura, Y., Ohbayashi, C., Okita, Y., Hayashi, Y., Yoshimura, M., 2011. MT1-MMP plays an important role in an invasive activity of malignant pleural mesothelioma cell. Experimental and Molecular Pathology 90, 91–96.

Faris, R.A., McEntire, K.D., Thompson, N.L., Hixson, D.C., 1990. Identification and characterization of a rat hepatic oncofetal membrane glycoprotein. Cancer Research 50, 4755–4763.

Fujito, T., Ikeda, W., Kakunaga, S., Minami, Y., Kajita, M., Sakamoto, Y., Monden, M., Takai, Y., 2005. Inhibition of cell movement and proliferation by cell–cell contact-induced interaction of Necl-5 with nectin-3. The Journal of Cell Biology 171, 165–173.

Golubovskaya, V.M., 2010. Focal adhesion kinase as a cancer therapy target. Anti-Cancer Agents in Medicinal Chemistry 10, 735–741.

Ikeda, W., Kakunaga, S., Itoh, S., Shingai, T., Takekuni, K., Satoh, K., Inoue, Y., Hamaguchi, A., Morimoto, K., Takeuchi, M., Imai, T., Takai, Y., 2003. Tage4/Nectin-like molecule-5 heterophilically trans-interacts with cell adhesion molecule Nectin-3 and enhances cell migration. The Journal of Biological Chemistry 278, 28167–28172.

Ikeda, W., Kakunaga, S., Takekuni, K., Shingai, T., Satoh, K., Morimoto, K., Takeuchi, M., Imai, T., Takai, Y., 2004. Nectin-like molecule-5/Tage4 enhances cell migration in an integrin-dependent, Nectin-3-independent manner. The Journal of Biological Chemistry 279, 18015–18025.

Kakunaga, S., Ikeda, W., Shingai, T., Fujito, T., Yamada, A., Minami, Y., Imai, T., Takai, Y., 2004. Enhancement of serum- and platelet-derived growth factor-induced cell proliferation by Necl-5/Tage4/poliovirus receptor/CD155 through the Ras–Raf–MEK–ERK signaling. The Journal of Biological Chemistry 279, 36419–36425.

Kerr, K.M., 2009. Pulmonary adenocarcinomas: classification and reporting. Histopathology 54, 12–27.

Koike, S., Horie, H., Ise, I., Okitsu, A., Yoshida, M., Iizuka, N., Takeuchi, K., Takegami, T., Nomoto, A., 1990. The poliovirus receptor protein is produced both as membrane-bound and secreted forms. The EMBO Journal 9, 3217–3224.

Lim, Y.P., Fowler, L.C., Hixson, D.C., Wehbe, T., Thompson, N.L., 1996. TuAg.1 is the liver isoform of the rat colon tumor-associated antigen pE4 and a member of the immunoglobulin-like supergene family. Cancer Research 56, 3934–3940.

Liotta, L.A., Kohn, E.C., 2001. The microenvironment of the tumour–host interface. Nature 411, 375–379.

Miyoshi, J., Takai, Y., 2007. Nectin and nectin-like molecules: biology and pathology. American Journal of Nephrology 27, 590–604.

Morimoto, K., Satoh-Yamaguchi, K., Hamaguchi, A., Inoue, Y., Takeuchi, M., Okada, M., Ikeda, W., Takai, Y., Imai, T., 2008. Interaction of cancer cells with platelets mediated by Necl-5/poliovirus receptor enhances cancer cell metastasis to the lungs. Oncogene 27, 264–273.

Nakai, R., Maniwa, Y., Tanaka, Y., Nishio, W., Yoshimura, M., Okita, Y., Ohbayashi, C., Satoh, N., Ogita, H., Takai, Y., Hayashi, Y., 2010. Overexpression of Necl-5 correlates with unfavorable prognosis in patients with lung adenocarcinoma. Cancer Science 101, 1326–1330.

Noguchi, M., Morikawa, A., Kawasaki, M., Matsuno, Y., Yamada, T., Hirohashi, S., Kondo, H., Shimosato, Y., 1995. Small adenocarcinoma of the lung. Histologic characteristics and prognosis. Cancer 75, 2844–2852.

Sato, T., Irie, K., Ooshio, T., Ikeda, W., Takai, Y., 2004. Involvement of heterophilic trans-interaction of Necl-5/Tage4/PVR/CD155 with nectin-3 in formation of nectin- and cadherin-based adherens junctions. Genes to Cells 9, 791–799.

Shioiri, M., Shida, T., Koda, K., Oda, K., Seike, K., Nishimura, M., Takano, S., Miyazaki, M., 2006. Slug expression is an independent prognostic parameter for poor survival in colorectal carcinoma patients. British Journal of Cancer 94, 1816–1822.

Sloan, K.E., Eustace, B.K., Stewart, J.K., Zehetmeier, C., Torella, C., Simeone, M., Roy, J.E., Unger, C., Louis, D.N., Ilag, L.L., Jay, D.G., 2004. CD155/PVR plays a key role in cell motility during tumor cell invasion and migration. BMC Cancer 4, 73.

Soltermann, A., Tischler, V., Arbogast, S., Braun, J., Probst-Hensch, N., Weder, W., Moch, H., Kristiansen, G., 2008. Prognostic significance of epithelial–mesenchymal and mesenchymal–epithelial transition protein expression in non-small cell lung cancer. Clinical Cancer Research 14, 7430–7437.

Takai, Y., Sasaki, T., Matozaki, T., 2001. Small GTP-binding proteins. Physiological Reviews 81, 153–208.

Takai, Y., Irie, K., Shimizu, K., Sakisaka, T., Ikeda, W., 2003. Nectins and nectin-like molecules: roles in cell adhesion, migration, and polarization. Cancer Science 94, 655–667.

Takai, Y., Miyoshi, J., Ikeda, W., Ogita, H., 2008. Nectins and nectin-like molecules: roles in contact inhibition of cell movement and proliferation. Nature Reviews. Molecular Cell Biology 9, 603–615.

Takata, M., Maniwa, Y., Doi, T., Tanaka, Y., Okada, K., Nishio, W., Ohbayashi, C., Yoshimura, M., Hayashi, Y., Okita, Y., 2007. Double-layered collagen gel hemisphere for cell invasion assay: successful visualization and quantification of cell invasion activity. Cell Communication & Adhesion 14, 157–167.

Thiery, J.P., 2002. Epithelial–mesenchymal transitions in tumour progression. Nature Reviews. Cancer 2, 442–454.

Tokunou, M., Niki, T., Eguchi, K., Iba, S., Tsuda, H., Yamada, T., Matsuno, Y., Kondo, H., Saitoh, Y., Imamura, H., Hirohashi, S., 2001. c-MET expression in myofibroblasts: role in autocrine activation and prognostic significance in lung adenocarcinoma. The American Journal of Pathology 158, 1451–1463.

Webb, D.J., Donais, K., Whitmore, L.A., Thomas, S.M., Turner, E.T., Parsons, J.P., Horwitz, A.F., 2004. FAK–Src signalling through paxillin, ERK and MLCK regulates adhesion disassembly. Nature Cell Biology 6, 154–161.

19. Trial of erlotinib and BKM120 in patients with advanced non small cell lung cancer previously sensitive to erlotinib; http://www.clinicaltrials.gov/ct2/show/NCT01487265 (7 March 2013, date last accessed).
20. Shukuya T, Takahashi T, Kaira R et al. Efficacy of gefitinib for non-adenocarcinoma non-small-cell lung cancer patients harboring epidermal growth factor receptor mutations: a pooled analysis of published reports. Cancer Sci 2011; 102: 1032–1037.
21. Weiss J, Sos ML, Seidel D et al. Frequent and focal FGFR1 amplification associates with therapeutically tractable FGFR1 dependency in squamous cell lung cancer. Sci Transl Med 2010; 2: 62ra93. Errata in: Sci Transl Med 2012; 4: 130er2. Sci Transl Med 2011; 3: 66er2.
22. National Cancer Institute. The Cancer Genome Atlas; updated 2011; http://cancergenome.nih.gov/ (22 November 2011, date last accessed).
23. Hammerman PS, Hayes DN, Wilkerson MD et al. Comprehensive genomic characterization of squamous cell lung cancers. Nature 2012; 489: 519–525.
24. Thomas R. Identifying clinically relevant cancer genome alterations in lung cancer: The Clinical Lung Cancer Genome Project initiative; updated 2010; http://www.abstractsonline.com/plan/ViewAbstract.aspx?mID=2626&sKey=9269f5cb-5ea2-48c1-996d-e95d7b1d265e&cKey=7983f06c-92c1-4149-bf81-f7b64bcd8288&mKey=%7BE69F27FB-E294-49DA-92AC-DFC241A99F23%7D (21 September 2011, date last accessed).
25. Arrieta O, Cardona AF, Federico Bramuglia G et al. Genotyping non-small cell lung cancer (NSCLC) in Latin America. J Thorac Oncol 2011; 6: 1955–1959.
26. National Comprehensive Cancer Network. Practice guidelines in oncology – version V.3.2012 (non-small-cell lung cancer); updated 2012; http://www.nccn.org/professionals/physician_gls/pdf/nscl.pdf (6 December 2011, date last accessed).
27. Balak MN, Gong Y, Riely GJ et al. Novel D761Y and common secondary T790M mutations in epidermal growth factor receptor-mutant lung adenocarcinomas with acquired resistance to kinase inhibitors. Clin Cancer Res 2006; 12: 6494–6501.
28. Kosaka T, Yatabe Y, Endoh H et al. Analysis of epidermal growth factor receptor gene mutation in patients with non-small cell lung cancer and acquired resistance to gefitinib. Clin Cancer Res 2006; 12: 5764–5769.

Annals of Oncology 24: 2376–2381, 2013
doi:10.1093/annonc/mdt230
Published online 20 June 2013

Solid tumor size on high-resolution computed tomography and maximum standardized uptake on positron emission tomography for new clinical T descriptors with T1 lung adenocarcinoma

Y. Tsutani[1], Y. Miyata[1], H. Nakayama[2], S. Okumura[3], S. Adachi[4], M. Yoshimura[5] & M. Okada[1]*

[1]Department of Surgical Oncology, Hiroshima University, Hiroshima; [2]Department of Thoracic Surgery, Kanagawa Cancer Center, Yokohama; [3]Department of Thoracic Surgery, Cancer Institute Hospital, Tokyo; [4]Departments of Radiology; [5]Thoracic Surgery, Hyogo Cancer Center, Akashi, Japan

Received 5 March 2013; revised 8 May 2013; accepted 10 May 2013

Background: To better describe clinical T descriptors using solid tumor size (the maximum dimension of the solid component of the tumor) on high-resolution computed tomography (HRCT) and maximum standardized uptake value (SUV_{max}) on F-18-fluorodeoxyglucose positron emission tomography/CT (FDG-PET/CT).

Patients and methods: We examined 610 consecutive patients with clinical stage IA lung adenocarcinoma who underwent complete resection. Recurrence-free survival (RFS) was assessed on the basis of whole tumor size (maximum dimension of the tumor), solid tumor size, or a combination of solid tumor size and SUV_{max}.

Results: RFS based on whole tumor size was not significantly different between patients with tumors measuring ≤2 cm and 2–3 cm ($P = 0.089$), whereas RFS based on solid tumor size was significantly different ($P < 0.0001$). We divided patients into four groups on the basis of solid tumor size and SUV_{max}: group 1: solid tumor size ≤2 cm, SUV_{max} ≤1.8; group 2: solid tumor size ≤2 cm, SUV_{max} >1.8; group 3: solid tumor size 2–3 cm, SUV_{max} ≤3.6; and group 4: solid tumor size 2–3 cm, SUV_{max} >3.6. Groups 2 and 3 were combined because they showed similar RFS each other. RFS was significantly different among these groups: group 1 versus groups 2 + 3, $P < 0.0001$; groups 2 + 3 versus group 4, $P = 0.019$.

Conclusions: Both solid tumor size on HRCT and SUV_{max} on FDG-PET/CT reflect prognosis well in patients with clinical stage IA lung adenocarcinoma and may support new clinical T descriptors.

Key words: lung adenocarcinoma, positron emission tomography, T descriptor, TNM classification

*Correspondence to: Prof. Morihito Okada, Department of Surgical Oncology, Research Institute for Radiation Biology and Medicine, Hiroshima University, 1-2-3-Kasumi, Minami-ku, Hiroshima City, Hiroshima 734-0037, Japan. Tel: +81-82-257-5869; Fax: +81-82-256-7109; E-mail: morihito@hiroshima-u.ac.jp

introduction

Adenocarcinoma is the most common histologic subtype of lung cancer in most countries, accounting for ~50% of all lung cancers [1]. The widespread use of low-dose helical computed tomography (CT) for screening tumors has increased the early detection rate for smaller non-small-cell lung cancer (NSCLC), particularly adenocarcinoma [2]. These tumors often comprise a nonsolid component presenting as ground-glass opacity (GGO) on high-resolution CT (HRCT) [3].

A GGO component is closely associated with a pathologic lepidic growth component [4]. Because lepidic growth components are considered to have little effect on patient survival [5], GGO components may also have little effect on patient survival. We previously demonstrated that solid tumor size excluding GGO component on HRCT had a greater predictive value for pathologic tumor invasiveness and prognosis compared with whole tumor size for clinical stage IA lung adenocarcinoma [3]. We have also observed that the maximum standardized uptake value (SUV_{max}) on 18F-fluoro-2-deoxyglucose (FDG) positron emission tomography (PET)/CT was an important preoperative factor for predicting the pathologic malignant grade and prognosis in lung adenocarcinoma [3, 6–9]. Both solid tumor size on HRCT and SUV_{max} on FDG-PET/CT were independent predictive factors for pathologic tumor invasiveness and prognosis [3, 9].

The tumor–node–metastasis (TNM) staging system for NSCLC is internationally accepted and used to determine the disease stage, which in turn guides disease management and determines prognosis [10]. Regarding clinical T descriptors, tumor size is usually measured as whole tumor size including solid and GGO components, without considering qualitative parameters such as SUV_{max} on PET/CT [11]. Here, we attempted to employ promising factors such as solid tumor size on HRCT and SUV_{max} on FDG-PET/CT as better clinical T descriptors of pathologic tumor invasiveness and prognosis compared with the present T descriptors based on whole tumor size.

patients and methods

patients

We enrolled 610 patients with clinical T1 N0 M0 stage IA lung adenocarcinoma from four institutions (Hiroshima University, Kanagawa Cancer Center, Cancer Institute Hospital, and Hyogo Cancer Center, Japan) between 1 August 2005 and 30 June 2010 to evaluate the significance of FDG-PET/CT. Patients with incompletely resected tumors (R1 or R2) and those with multiple tumors or previous lung surgeries were not included. This multicenter patient database was maintained prospectively and was retrospectively analyzed for this study.

HRCT and FDG-PET/CT followed by curative R0 resection were carried out for all patients staged according to the TNM Classification of Malignant Tumours, 7th Edition [10]. Mediastinoscopy and endobronchial ultrasonography were not routinely carried out, because all patients had undergone preoperative HRCT and FDG-PET/CT. HRCT revealed no enlargement of mediastinal or hilar lymph nodes measuring >1 cm; FDG-PET/CT showed no accumulation of an SUV_{max} of >1.5 in these lymph nodes.

Segmentectomy was considered for patients with clinical stage IA tumors that could be completely resected with ample surgical margins. No lymph node metastasis was intraoperatively confirmed using rapid frozen sections for enlarged lymph nodes or lymph nodes that were suspected with disease in the thoracic cavity. In cases of apparent or suspected nodal metastasis, lobectomy was chosen. Systematic lymphadenectomy including hilar and mediastinal node dissection can be carried out during segmentectomy but not during wedge resection. Therefore, wedge resection was carried out for tumors mainly exhibiting a GGO component on HRCT. Patients who had pathologically confirmed lymph node metastasis (N1 or N2) underwent platinum-based chemotherapy after surgery.

Surgically resected tumors were fixed with 10% formalin and embedded in paraffin. Consecutive 4-μm sections had been cut and evaluated histopathologically using hematoxylin and eosin and elastic van Gieson staining. Pathologic findings were evaluated by independent pathologists from each institution.

The inclusion criteria were preoperative staging determined by HRCT and FDG-PET/CT, curative surgery without neoadjuvant chemotherapy or radiotherapy, and a definitive histopathologic diagnosis of lung adenocarcinoma. This study was approved by the institutional review boards of the participating institutions. The requirement for informed consent from individual patients was waived, because this study was a retrospective review of a patient database.

HRCT

See supplementary File, available at *Annals of Oncology* online.

FDG-PET/CT

See supplementary File, available at *Annals of Oncology* online.

follow-up evaluations

All patients who underwent lung resection were followed up from the day of surgery. Patients underwent postoperative follow-up procedures, including physical examinations and chest roentgenography every 3 months and chest and abdominal CT every 6 months, for the first 2 years. Subsequently, they underwent physical examinations and chest roentgenography every 6 months and chest CT every year.

statistical analysis

Results were presented as numbers (%) or median values unless otherwise stated. The χ^2 test for categorical variables was used to compare frequencies and the Fisher's exact test was used for small samples. Receiver operating characteristic (ROC) curves of SUV_{max} for predicting pathologic tumor invasiveness were generated to determine the cutoff value yielding optimal sensitivity and specificity. Recurrence-free survival (RFS) was defined as the time from the day of surgery until the first adverse event (relapse or death from any cause) or until the last follow-up. Kaplan–Meier curves were used to assess RFS duration, and a log-rank test was used to assess differences in RFS. Statistical Package for the Social Sciences (SPSS) software (version 10.5; SPSS, Inc., Chicago, IL, USA) was used for statistical analysis. The level of statistical significance was set at $P < 0.05$.

results

Table 1 summarizes the characteristics of the 610 patients evaluated in this study. Of these, 376, 97, and 137 underwent lobectomy, segmentectomy, and wedge resection, respectively. No 30-day postoperative mortality was observed in this

doi:10.1093/annonc/mdt230

population. The median follow-up period following surgery was 41.5 (1.5–75.7) months, during which tumors recurred in 58 patients. There were 22 local-only recurrences, including mediastinal lymph node metastasis, and 36 distant ± local recurrences. There was no difference in the incidences of local-only recurrences between patients who underwent lobectomy and those who underwent sublobar resection [16 of 376 (4.3%) and 6 of 234 (2.6%), respectively, $P = 0.37$].

The median whole tumor and solid tumor sizes on HRCT were 2.0 and 1.2 cm, respectively. Lymphatic, vascular, and pleural invasions were detected in 89 (14.6%), 104 (17.0%), and 66 (10.8%) patients, respectively, and lymph nodes were involved in 41 (6.7%) patients. Three were intrapulmonary, 17 were hilar, and 21 were mediastinal lymph node metastases.

No significant difference in RFS was observed between patients with a whole tumor size of ≤2.0 cm (3-year RFS rate: 91.0%) and those with a whole tumor size of 2–3 cm (3-year RFS rate: 86.3%; $P = 0.089$; Figure 1A). In contrast, a significant difference in RFS was observed between patients with a solid tumor size ≤2.0 cm (3-year RFS rate: 91.7%) and those with a solid tumor size of 2–3 cm (3-year RFS rate: 77.6%, $P < 0.0001$; Figure 1B).

We generated ROC curves to decide the optimal cutoff values of SUV_{max} for predicting pathologic tumor invasiveness (lymphatic, vascular, or pleural invasion) in each solid tumor size group (solid tumor size of ≤2.0 cm or 2–3 cm). These ROC curves identified optimal SUV_{max} cutoff values of 1.8 [area under the curve (AUC) = 0.85; sensitivity = 77.3%; specificity = 79.3%] for a solid tumor size ≤2.0 cm and 3.6 (AUC = 0.79; sensitivity = 73.8%; specificity = 77.6%) for a solid tumor size of 2–3 cm (supplementary Figure S1A and B, available at *Annals of Oncology* online). Therefore, the patient population was subdivided into four groups on the basis of solid tumor size and optimal SUV_{max} cutoff values: group 1: solid tumor size ≤2.0 cm and SUV_{max} ≤1.8; group 2: solid tumor size ≤2.0 cm and SUV_{max} >1.8; group 3: solid tumor size 2–3 cm and SUV_{max} ≤3.6; and group 4: solid tumor size 2–3 cm and SUV_{max} >3.6.

The 3-year RFSs for groups 1, 2, 3, and 4 were 95.6%, 83.3%, 85.0%, and 70.8%, respectively (group 1 versus 2, $P < 0.0001$; group 2 versus 3, $P = 0.87$; group 2 versus 4, $P = 0.030$; Figure 2A). Because groups 2 and 3 had similar survival rates, we proposed the new clinical T descriptors as follows: proposed c-T1a (group 1): solid tumor size ≤2.0 cm and SUV_{max} ≤1.8; proposed c-T1b (groups 2 + 3): solid tumor size ≤2.0 cm and SUV_{max} >1.8, solid tumor size 2–3 cm and SUV_{max} ≤3.6; proposed c-T1c (group 4), solid tumor size 2–3 cm and SUV_{max} >3.6.

Table 1. Patient characteristics ($N = 610$)

Age (year)	66 (31–89)
Gender	
Male	268 (43.9%)
Whole tumor size (cm)	2.0 (0.6–3.0)
Solid tumor size (cm)	1.2 (0–3.0)
SUV_{max}	1.6 (0–17)
Clinical T descriptor	
T1a	354 (58.0%)
T1b	256 (42.0%)
Procedures	
Lobectomy	376 (61.6%)
Segmentectomy	97 (15.9%)
Wedge resection	137 (22.5%)
Lymphatic invasion	
Positive	89 (14.6%)
Vascular invasion	
Positive	104 (17.0%)
Pleural invasion	
Positive	66 (10.8%)
Lymph node metastasis	
Positive	41 (6.7%)

SUV_{max}: maximum standardized uptake value.

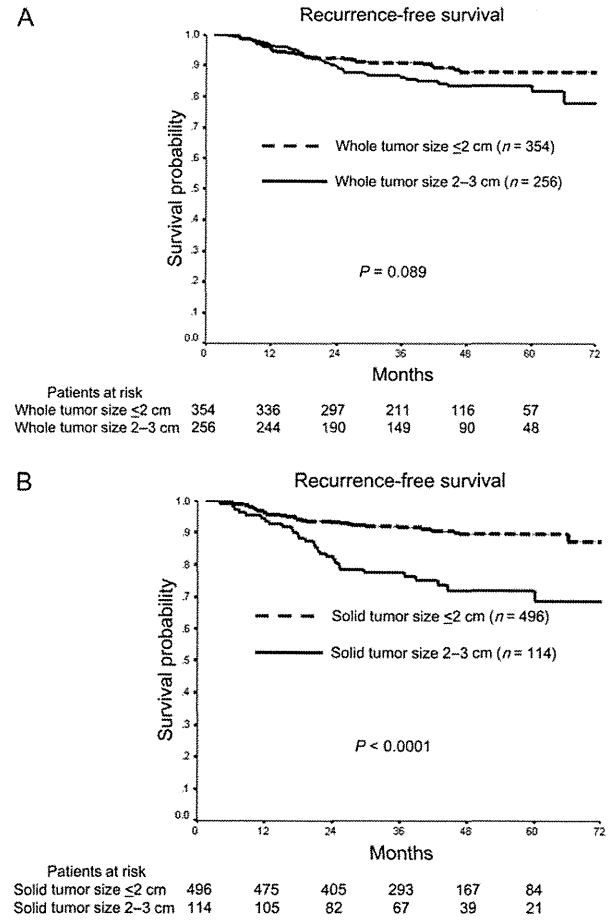

Figure 1. Recurrence-free survival (RFS) curves for patients with clinical stage IA lung adenocarcinoma based on whole tumor size (A) and solid tumor size (B). (A) Three-year RFS rates of 91.0% (mean RFS, 69.2 months; 95% confidence interval [CI]: 67.1–71.2 months) and 86.3% (mean RFS, 65.4 months; 95% CI: 62.7–68.1 months) were identified for patients with whole tumor size of ≤2 cm and those with whole tumor sizes of 2–3 cm, respectively ($P = 0.089$). (B) Three-year RFS rates of 91.7% (mean RFS, 69.8 months; 95% CI: 68.2–71.5 months) and 77.6% (mean RFS, 59.4 months; 95% CI: 54.6–64.2 months) were found for patients with solid tumor size of ≤2 cm and those with solid tumor size of 2–3 cm, respectively ($P < 0.0001$).

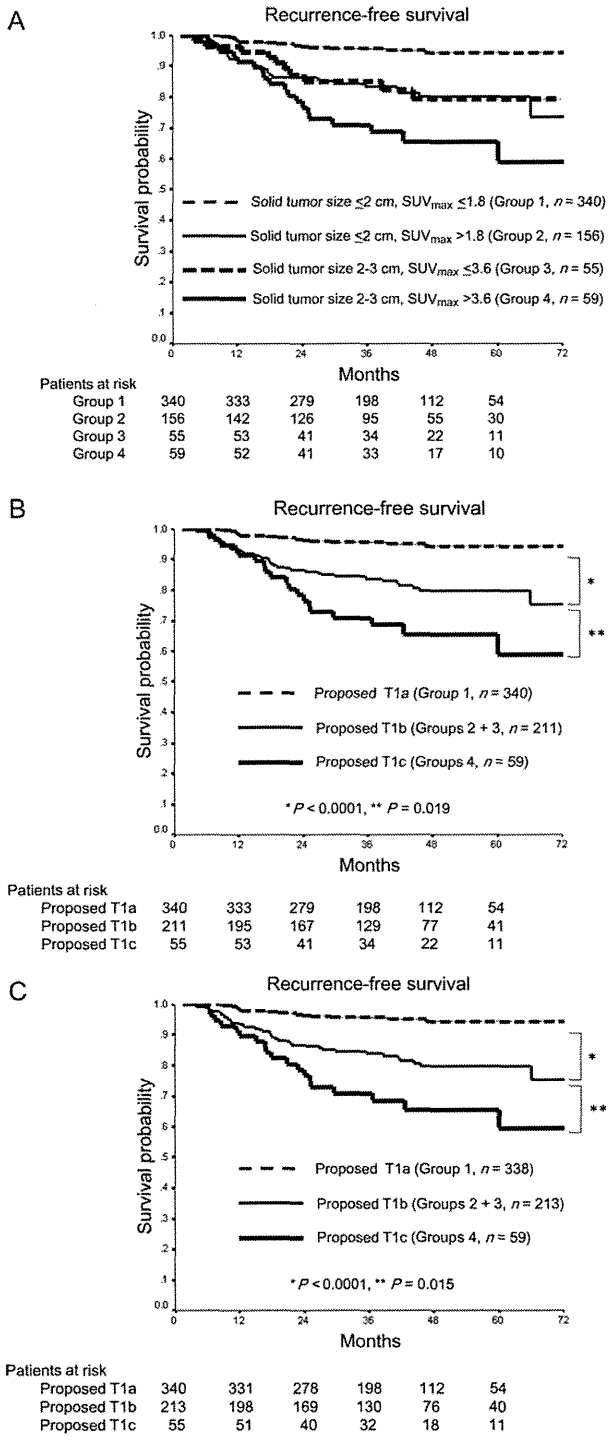

Figure 2. *Recurrence-free survival (RFS) curves for patients with clinical stage IA lung adenocarcinoma based on solid tumor size and maximum standardized uptake value (SUV_{max}). (A) Group 1: solid tumor size ≤2 cm, SUV_{max} ≤1.8; group 2: solid tumor size ≤2 cm, SUV_{max} >1.8; group 3, solid tumor size 2–3 cm, SUV_{max} ≤3.6; group 4, solid tumor size 2–3 cm, SUV_{max} >3.6. Three-year RFSs for groups 1, 2, 3, and 4 were, respectively, 95.6% (mean RFS, 72.7 months; 95% confidence interval [CI], 71.2–74.1 months), 83.3% (mean RFS, 62.4 months; 95% CI: 58.7–66.2 months), 85.0% (mean RFS, 61.4 months; 95% CI: 55.7–67.0 months), and 70.8% (mean RFS, 55.2 months; 95% CI: 48.1–62.3 months). Group 1 versus 2, $P < 0.0001$; group 2 versus 3, $P = 0.87$; group 2 versus 4, $P = 0.030$. (B) Proposed c-T1a = group 1 in (A); proposed c-T1b = groups 2 + 3 in (A); proposed c-T1c = group 4 in (A); SUV_{max} was based on revised values. Three-year RFSs for proposed c-T1a, c-T1b, and c-T1c were 95.6% (mean RFS, 72.7 months; 95% CI: 71.2–74.1 months), 83.7% (mean RFS, 62.7 months; 95% CI: 59.5–65.8 months), and 70.8% (mean RFS, 55.2 months; 95% CI: 48.1–62.3 months), respectively. There were significant differences in RFS between proposed clinical T descriptors: proposed c-T1a versus proposed c-T1b, $P < 0.0001$; proposed c-T1b versus proposed c-T1c, $P = 0.019$. (C) Groups were the same as in (B), except SUV_{max} was based on original values. Three-year RFS results for proposed c-T1a, c-T1b, and c-T1c were, respectively, 95.6% (mean = 72.7 months; 95% CI: 71.2–74.1 months), 83.9% (mean = 62.8 months; 95% CI: 59.7–65.9 months), and 70.7% (mean = 55.0 months; 95% CI; 47.9–62.2 months). There were significant differences in RFS between proposed clinical T descriptors: proposed c-T1a versus proposed c-T1b, $P < 0.0001$; proposed c-T1b versus proposed c-T1c, $P = 0.015$.*

The 3-year RFSs for proposed c-T1a (group 1), c-T1b (groups 2 + 3), and c-T1c (group 4) were 95.6%, 83.7%, and 70.8%, respectively. There were significant differences in RFS between the proposed clinical T descriptors: proposed c-T1a (group 1) versus proposed c-T1b (groups 2 + 3), $P < 0.0001$; proposed c-T1b (groups 2 + 3) versus proposed c-T1c (group 4), $P = 0.019$ (Figure 2B). The incidences of local-only recurrences were significantly different among the proposed T descriptors [2 of 340 (0.6%) in proposed T1a (group 1), 13 of 211 (6.2%) in proposed T1b (groups 2 + 3), and 7 of 59 (11.9%) in proposed T1c (group 4), respectively, $P < 0.001$].

There were also significant differences in pathologic findings (lymphatic, vascular, and pleural invasion, and also lymph node metastasis) among the proposed clinical T descriptors (all $P < 0.001$; Table 2).

Table 3 summarizes the differences in the distributions between the present T descriptors and our proposed descriptors. Among those with presently defined T1a tumors, 123 of 354 (34.7%) were upgraded to proposed T1b (groups 2 + 3). Among those with presently defined T1b tumors, 59 of 256 (23.0%) were upgraded to proposed T1c (group 4), while 109 of 256 (42.6%) with presently defined T1b tumors were downgraded to proposed T1a (group 1).

When we used the original SUV_{max} values before revision, the 3-year RFSs for proposed c-T1a (group 1), c-T1b (groups 2 + 3), and c-T1c (group 4) were 95.6%, 83.9%, and 70.7%, respectively. Significant differences in RFS remained between the proposed clinical T descriptors: proposed c-T1a (group 1) versus proposed c-T1b (groups 2 + 3), $P < 0.0001$; proposed c-T1b (groups 2 + 3) versus proposed c-T1c (group 4), $P = 0.015$ (Figure 2C).

discussion

In this study, the comparison between the present clinical T descriptors based on whole tumor size and solid tumor size on HRCT showed that the latter could be successfully used to subdivide the patients into different prognosis groups, indicating that GGO components had little effect on patient survival. We previously reported that solid tumor size on HRCT predicted pathologic tumor invasiveness better than whole tumor size for clinical stage IA lung adenocarcinoma [3].

doi:10.1093/annonc/mdt230

Recently, another report also showed that excluding a GGO component resulted in improved prognostic performance for recurrence and pathologic vessel invasion in T1–2 N0 M0 lung adenocarcinoma [12]. Our results were consistent with those of previous reports, and the importance of solid tumor size when excluding a GGO component for predicting survival was confirmed. Solid tumor size excluding a GGO component should be used instead of whole tumor size to determine T descriptors in lung adenocarcinoma.

SUV_{max} on FDG-PET/CT was indicated as a prognostic factor for NSCLC [13], particularly for lung adenocarcinoma [3, 6–9]. SUV_{max} also has the potential to be a T descriptor as a quantitative factor for predicting pathologic tumor invasiveness and prognosis. One limitation of applying SUV_{max} to T descriptor is the cutoff value. In a multicenter study, variations in SUV quantitation resulting from differences in the quality of PET/CT scanners are disadvantages [14]. To adjust for these variations, we used an anthropomorphic body phantom that conformed to the National Electrical Manufacturers Association standards [15]. To determine the optimal cutoff values, we used ROC curves for SUV_{max} to predict pathologic tumor invasiveness (lymphatic, vascular, or pleural invasion). We determined cutoff values of 1.8 and 3.6 for the solid tumor size of ≤2 and 2–3 cm, respectively. Interestingly, the predictive capabilities of pathologic tumor invasiveness based on these cutoff values were quite similar in each group based on solid tumor size (sensitivity = 73.8%–77.3%; specificity = 77.6%–79.7%). This suggested that these cutoff values were reasonable.

Regarding prognosis, patients with the solid tumor size of ≤2 cm and SUV_{max} of >1.8 had similar RFS results, compared with those with the solid tumor size of >2 cm and SUV_{max} of ≤3.6. This was also an interesting finding. Based on this, we proposed the following new T descriptors: proposed T1a: solid tumor size ≤2 cm and SUV_{max} ≤1.8; proposed T1b: solid tumor size ≤2 cm and SUV_{max} >1.8 or solid tumor size 2–3 cm and SUV_{max} ≤3.6; and proposed T1c: solid tumor size 2–3 cm and SUV_{max} >3.6. This indicated that high SUV_{max} tumors could be upgraded. Based on our proposed T descriptors, RFSs and pathologic tumor malignancies were significantly different among these groups.

Comparing our proposed T descriptors with present descriptors, 34.7% present T1a tumors were upgraded to proposed T1b, 23.0% present T1b tumors were upgraded to proposed T1c, and 42.6% present T1b tumors were downgraded to proposed T1a. This indicated that the present T descriptors did not successfully represent tumor malignancies and prognosis, which may be due to the heterogeneities of lung adenocarcinomas. Solid tumor size on HRCT and SUV_{max} on FDG-PET/CT could explain these heterogeneities of lung adenocarcinomas as preoperative radiologic findings.

For clinical practice, it was important that using the original SUV_{max} retained the prognostic differences among the groups based on our proposed new T descriptors. When the original SUV_{max} was used, our proposed T descriptors could successfully subdivide our patients into different prognostic groups. To confirm our proposed T descriptors, a validation study with another cohort and international standardization protocols of FDG-PET/CT are needed. These were limitations of our study. Another limitation was that our database did not include tumors with a whole tumor size of >3 cm. Therefore, whether our proposed clinical T1c can be regarded as T2a is unknown. Further studies including large tumors are warranted. We used two-dimensional measurements of tumor sizes for this study. Three-dimensional measurements such as metabolic tumor volume using HRCT and FDG-PET/CT may also have a potential to be considered as new T descriptors [16].

Table 2. Pathologic findings based on our newly proposed clinical T descriptors

	Proposed T1a ($N = 340$)	Proposed T1b ($N = 211$)	Proposed T1c ($N = 59$)	*P*-value
Lymphatic invasion	12 (3.5%)	52 (24.6%)	25 (43.4%)	<0.001
Vascular invasion	8 (2.4%)	59 (28.0%)	37 (62.7%)	<0.001
Pleural invasion	6 (1.8%)	36 (17.1%)	24 (40.7%)	<0.001
Lymph node metastasis	4 (1.2%)	27 (12.8%)	10 (16.9%)	<0.001

Table 3. Differences in distributions between the present T descriptors and our proposed clinical T descriptors

	Present T1a ($N = 354$)	Present T1b ($N = 256$)
Proposed T1a ($N = 340$)	231	109
Proposed T1b ($N = 211$)	123	88
Proposed T1c ($N = 59$)	0	59

Sublobar resection for treating small lung cancer has under debate for a long time [8, 17–20]. Selecting optimal candidates for sublobar resection is important. Our proposed new T descriptors may contribute to selecting patients for sublobar resection. Patients with our newly proposed T1a tumors may be good candidates for sublobar resection, because they have less pathologic invasiveness such as lymphatic, vascular, or pleural invasion, and lymph node metastases.

In conclusion, T descriptors should be based on solid tumor size on HRCT, which is more useful for predicting pathologic tumor invasiveness and prognosis than whole tumor size. Furthermore, SUV_{max} on FDG-PET/CT, which also successfully predicts tumor invasiveness and prognosis of early lung adenocarcinoma, has adequate potential to be a new T descriptor. The combination of solid tumor size and SUV_{max} predicts the survival better than solid tumor size alone and may contribute to decision-making for sublobar resection in patients with clinical stage IA lung adenocarcinoma. We hope that solid tumor size on HRCT and SUV_{max} on FDG-PET/CT will be taken into account in the next revisions for T descriptors.

disclosure

The authors have declared no conflicts of interest.

references

1. Curado MP, Edwards B, Shin HR et al Cancer Incidence in Five Continents, Vol. IX. Lyon: IARC Scientific Publications 2007.
2. National Lung Screening Trial Research Team, Aberle DR, Adams AM et al Reduced lung-cancer mortality with low-dose computed tomographic screening. N Engl J Med 2011; 365: 395–409.
3. Tsutani Y, Miyata Y, Nakayama H et al Prognostic significance of using solid versus whole tumor size on high-resolution computed tomography for predicting the pathological malignant grade of tumors in clinical stage IA lung adenocarcinoma: a multicenter study. J Thorac Cardiovasc Surg 2012; 143: 607–612.
4. Jang HJ, Lee KS, Kwon OJ et al Bronchioloalveolar carcinoma: focal area of ground-glass attenuation at thin-section CT as an early sign. Radiology 1996; 199: 485–488.
5. Yoshizawa A, Motoi N, Riely GJ et al Impact of proposed IASLC/ATS/ERS classification of lung adenocarcinoma: prognostic subgroups and implications for further revision of staging based on analysis of 514 stage I cases. Mod Pathol 2011; 24: 653–664.
6. Okada M, Nakayama H, Okumura S et al Multicenter analysis of high-resolution computed tomography and positron emission tomography/computed tomography findings to choose therapeutic strategies for clinical stage IA lung adenocarcinoma. J Thorac Cardiovasc Surg 2011; 141: 1384–1391.
7. Tsutani Y, Miyata Y, Misumi K et al Difference in prognostic significance of maximum standardized uptake value on [18F]-fluoro-2deoxyglucose positron emission tomography between adenocarcinoma and squamous cell carcinoma of the lung. Jpn J Clin Oncol 2011; 41: 890–896.
8. Tsutani Y, Miyata Y, Nakayama H et al Prediction of pathologic node-negative clinical stage IA lung adenocarcinoma for optimal candidates undergoing sublobar resection. J Thorac Cardiovasc Surg 2012; 144: 1365–1371.
9. Tsutani Y, Miyata Y, Yamanaka T et al Solid tumors versus mixed tumors with a ground-glass opacity component in patients with clinical stage IA lung adenocarcinoma: prognostic comparison using high-resolution computed tomography findings. J Thorac Cardiovasc Surg 2012 December 12 [pub ahead of print], doi: 10.1016/j.jtcvs.2012.11.019.
10. Goldstraw P, Crowley J, Chansky K et al International Association for the Study of Lung Cancer International Staging Committee; Participating Institutions. The IASLC Lung Cancer Staging Project: proposals for the revision of the TNM stage groupings in the forthcoming (seventh) edition of the TNM Classification of Malignant Tumours. J Thorac Oncol 2007; 2: 706–714.
11. Rami-Porta R, Ball D, Crowley J et al The IASLC Lung Cancer Staging Project: proposals for the revision of the T descriptor in the forthcoming (seventh) edition of the TNM classification for lung cancer. J Thorac Oncol 2007; 2: 593–602.
12. Murakawa T, Konoeda C, Ito T et al The ground glass opacity component can be eliminated from the T-factor assessment of lung adenocarcinoma. Eur J Cardiothorac Surg 2013; 43: 925–932.
13. Cerfolio RJ, Bryant AS, Ohja B et al The maximum standardized uptake values on positron emission tomography of a non-small cell lung cancer predict stage, recurrence, and survival. J Thorac Cardiovasc Surg 2005; 130: 151–159.
14. Westerterp M, Pruim J, Oyen W et al Quantification of FDG PET studies using standardized uptake values in multicenter trials: effects of image reconstruction, resolution and ROI definition parameters. Eur J Nucl Med Mol Imaging 2007; 34: 392–404.
15. Mawlawi O, Podoloff DA, Kohlmyer S et al Performance characteristics of a newly developed PET/CT scanner using NEMA standards in 2D and 3D modes. J Nucl Med 2004; 45: 1734–1742.
16. Lee P, Bazan JG, Lavori PW et al Metabolic tumor volume is an independent prognostic factor in patients treated definitively for non-small cell lung cancer. Clin Lung Cancer 2012; 13: 52–58.
17. Ginsberg RH, Rubinstein LV. Randomized trial of lobectomy versus limited resection for T1N0 non-small cell lung cancer. Lung Cancer Study Group. Ann Thorac Surg 1995; 60: 615–623.
18. Okada M, Koike T, Higashiyama M et al Radical sublobar resection for small-sized non-small cell lung cancer: a multicenter study. J Thorac Cardiovasc Surg 2006; 132: 769–775.
19. Okada M, Tsutani Y, Ikeda T et al Radical hybrid video-assisted thoracic segmentectomy: long-term results of minimally invasive anatomical sublobar resection for treating lung cancer. Interact Cardiovasc Thorac Surg 2012; 14: 5–11.
20. Tsutani Y, Miyata Y, Nakayama H et al Oncologic outcomes of segmentectomy compared with lobectomy for clinical stage IA lung adenocarcinoma: propensity score-matched analysis in a multicenter study. J Thorac Cardiovasc Surg. 2013 March 8 [epub ahead of print], doi: 10.1016/j.jtcvs.2013.02.008.

肺血栓塞栓症(肺動脈血栓塞栓症)・気胸

山下素弘* 新海 哲**

要旨

・肺血栓塞栓症はがん患者の4～20%にみられ，その発症は予測困難で，臨床の現場では術後のみならず内科的治療の場でも問題となることが認識され始めている。発症すると急激な転帰となることも多い。
・臨床上のポイントとして，①がん治療を入院で行う患者では肺血栓塞栓症を念頭に置いたリスク評価と予防で発症頻度を少なくできる，②本症が疑われる際には造影CTが有用で迅速な初期対応で救命できる頻度も高くなる，③肺血栓塞栓症の治療法は肺動脈血管床の減少により生じる右心負荷が重症度と関連する，④具体的治療の選択には本疾患予防・診断・治療に関するガイドラインの活用が望まれる。
・気胸は緊張性気胸と血気胸で緊急を要するが，⑤診断は理学的初見や胸部X線写真で比較的容易に診断できる，⑥初期治療では胸腔ドレナージを行うことで呼吸循環動態は安定化できる場合が多い，初期治療後に患者の病態に応じた対策が必要となる。

はじめに

肺動脈血栓塞栓症(pulmonary thromboembolism；PE)を含む静脈血栓症(venous thromboembolism；VTE)は，日本ではこれまでまれな疾患と考えられていたが，欧米では虚血性心疾患，脳血管障害と並んで3大血管疾患としてとらえられている。高齢社会，食生活の欧米化，診断率の向上などにより，わが国においてもPEは確実に増加してきておりまれな疾患ではない。特に担がん患者の4～20%にVTEがみられ，また癌分子標的薬や血管新生阻害薬の登場による副作用や治療療養期間の長期化により，欧米ではがん患者の主な死因の一つにあげられている[1～3]。

わが国でもVTEはがんに対する治療上，特に周術期においては重要な危険因子であることが認識されてきているが，非観血的治療でのリスクの認識は少ないのが現状である。2009年に発表されたわが国でのVTEに対する診断・治療・予防に関するガイドライン[3]を中心に，欧米での知見も加えまとめた。また，気胸についてもオンコロジック・エマージェンシーにもなり得る疾患であり，併せて報告する。

背景・疫学的事項

担がん患者にVTEの発生頻度が高いことはよく知られており，その背景として腫瘍による血流

*独立行政法人国立病院機構四国がんセンター 胸部外科 **同 院長〔〒791-0280 松山市南梅本町甲160〕
YAMASHITA Motohiro, SHINKAI Tetsu

表1 急性肺動脈血栓塞栓症の臨床重症度分類

	血行動態	心エコー上右心不可所見
Cardiac arrest, collapse	心停止あるいは循環虚脱	あり
Massive	不安定 ショックあるいは低血圧*	あり
Submassive	安定(上記以外)	あり
Non-massive	安定(上記以外)	なし

*低血圧の定義：新たに出現した不整脈，脱水，敗血症によらず，15分以上継続する収縮期圧<90 mmHgあるいは≥40 mmHgの血圧低下

の停滞，血管内皮障害，生体内での凝固機能の亢進状態があげられる[4]。腫瘍の存在部位では腹部悪性腫瘍や脳腫瘍のみならず，血液悪性疾患の治療においてもVTE発生の頻度が高いとされており，がん患者の4～20%に症状を認めるVTEが発生しているとの報告がある。また，がん治療に伴う中心静脈カテーテルや治療薬剤，手術もVTE発症の大きな危険因子であるだけでなく，手術後やがんの進行に伴うADLの低下，長期臥床，脱水，炎症・感染症も危険因子となる。

臨床症状

発症状況では，安静解除後の起立・歩行や排便・排尿の際に発症することが多いのが特徴である。息切れはよくみられる症状であるが，VTEに特異的なものはなく，徐々にみられる労作時の息切れから，突然の呼吸困難に引き続き失神・ショック・心停止に至るものまで，さまざまである。頻呼吸，右心負荷による頻脈・低血圧も比較的多い症状であるが，他の疾患では説明できない呼吸困難では，本症も鑑別にあげられる。血栓塞栓による肺動脈内の血管床の減少に応じて生じる右心負荷が重症度と関連し，ショック状態や心停止することもまれではなく，特に術後の急性PEの死亡率は高い。

診断と重症度

経過を含めた症状から本疾患を疑うことが大切で，本疾患を疑えばまず造影CTを行い，肺動脈内の血流欠損像が決め手となる。誘引があり本症が疑われる場合には迅速に検査を進めることが大切である。造影CTで肺動脈内の血栓の検索を行うと同時に，PEの起因血栓の検索として下肢骨盤内静脈の造影CTや下肢の静脈エコー検査を行うことは，再発や重症化のリスクも評価でき，後述のinferior vena cava(IVC)フィルター挿入の必要性判断の参考とできる。

右心負荷の程度の判断として心電図検査，心エコー検査が有用で，バイタルサインとともに重症度分類に役立つ(表1)。血液検査ではDダイマーの上昇が役立つが，術後の発症では手術による影響かどうかの判断が求められる。

動脈血ガス分析では低炭酸ガス血症，低酸素血症，呼吸性アルカローシスを呈することが多く，肺胞気-動脈血酸素分圧格差($AaDO_2$)の開大もみられることが多い。経皮酸素分圧(SpO_2)の継時的モニターは，非侵襲的に低酸素血症の状況を簡便に把握できスクリーニングの一つとして役立つ。

予防と治療

1 予防

本疾患では予防に勝る治療法はないといって過

表2 静脈血栓塞栓症予防ガイドライン

レベル	下腿 DVT (%)	症候性 PE (%)	致死的 PE (%)	ACCP 予防法	わが国の推奨予防法
低リスク	2	0.2	0.002	早期離床	早期離床
中リスク	10～20	1～2	0.1～0.4	ES, IPC, LDH, or LMWH	ES or IPC
高リスク	20～40	2～4	0.4～1.0	IPC, LDH, or LMWH	IPC or LDH
最高リスク	40～80	4～10	0.2～5	LMWH, ES+LDH, or IPC+LDH	ES+LDH, or IPC+LDH

ACCP：American College of Chest Physicians，ES：弾性ストッキング，IPC：間欠的空気圧迫法，LDH：低用量未分画ヘパリン，LMWH：低分子量ヘパリン

(文献[6]より引用し一部改変)

言ではない。欧米での予防ガイドラインを参考に，わが国でも作成された VTE に対する診断・治療・予防に関するガイドライン[3]でも，リスクに応じた予防法が推奨されている。2012 年には American College of Chest Physicians(ACCP)[5]から，患者の状態に応じた詳細な予防・治療法が提唱されている(表 2)。

予防法の基本は，歩行を中心とする下肢の積極的運動である。下肢を自動的あるいは他動的に動かしたり，マッサージすることは，下腿のポンプ機能を活性化し下肢の静脈うっ滞を減少させる。弾性ストッキングは出血の合併症がなく，安価で簡便方法であるメリットがあり，中リスクの患者で有効性が高い。高リスク以上での弾性ストッキング単独使用効果は弱く，ほかの予防法と併用すべきである。間欠的空気圧迫法(intermittent pneumatic compression；IPC)は，高リスクで特に出血リスクの高い症例で有用である。下肢深部静脈血栓症が疑われたり既往を有する場合は，PE を誘発することもあり注意が必要となる。

抗凝固療法には未分画ヘパリン，ワルファリン，低分子ヘパリン，凝固 Xa 因子阻害薬(フォンダパリヌクス)がある。未分画ヘパリンの具体的使用法はやや煩雑で成書に委ねるが[3,5,6]，出血のリスクも評価して使用すれば最高リスク症例でも有効である。ワルファリンは調節に時間を要するが，わが国では prothrombin time-international normalized ratio(PT-INR)を 1.5～2.5 に目標としてコントロールすることが推奨されている。低分子ヘパリンやフォンダパリヌクスは，モニタリングの必要がなく 1 日 1～2 回の皮下投与で済むため，欧米では本予防薬の中心となっているが，わが国では保険適用が限られている。

2 治療

急性 PE の基本的病態は急性呼吸循環不全で，早期診断・早期治療がもっとも重要となる。急性期を乗り切れば比較的予後は良好で，循環動態が安定すれば再発に留意し VTE 対策が必要となる(図 1)。薬物による抗血栓療法が中心で，まず行われる方法は抗凝固療法である。出血リスクを考慮し，IVC フィルターや血栓溶解療法のほか，カテーテル治療により薬物治療効果を補うこともある。最重症例では経皮的心肺補助(percutaneous cardiopulmonary support；PCPS)や場合によっては外科的血栓摘除術も選択すべきであるが，施設の状況や個々の患者の病態に合わせた総合的判断が必要となる。

発症早期の死亡率は高いため，呼吸循環管理は極めて重要になる。呼吸不全としては，低炭酸ガス血症を伴う低酸素血症で，動脈血酸素分圧(PaO_2) 60 Torr 以上を保つよう酸素を投与する。

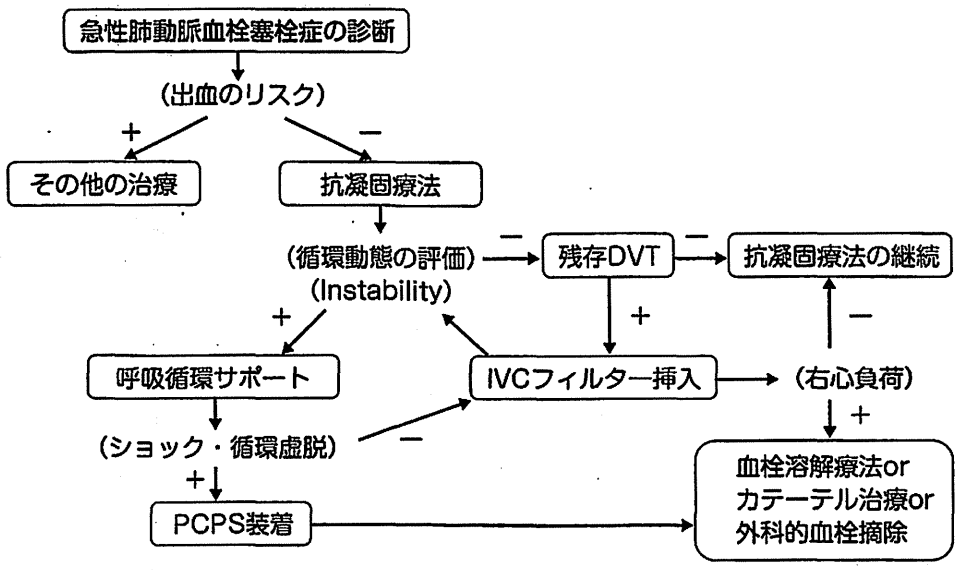

図1 急性肺動脈血栓塞栓症の治療アルゴリズム

DVT : deep vein thrombosis, IVC : inferior vena cava,
PCPS : percutaneous cardiopulmonary support

十分な血液酸素化が得られなければ人工換気を行う。循環動態としては，肺血管床の閉塞による右心不全，肺高血圧症が主体であるが，右心拍出量の極端な低下は左心拍出量の低下に直結しショック・循環虚脱を呈する。肺動脈拡張作用を有する薬剤(ドブタミンが第一選択薬，ドーパミン，フォスフォジエステラーゼⅢ阻害薬)やノルエピネフリンが有効であろう。心停止で発症した症例や薬物療法に反応が悪い症例では，PCPS装置の導入が勧められ手術による血栓摘除術も選択肢となる。

1）初期薬物治療

抗凝固療法の第一選択は未分画ヘパリンであり，出血傾向などの禁忌でない限り使用すべきである。本症が強く疑われる場合や確定診断に時間が掛かる場合には，疑診段階でも初期治療としてヘパリンを投与しても良い。まず5000単位(あるいは80単位/kg)を静注し，以後活性化部分トロンボプラスチン時間(activated partial thromboplastin time；APTT)をコントロールの1.5〜2.5倍となるよう持続点滴で調整し，ワルファリンの内服に移行する。

血栓溶解療法は，右心機能障害を有する場合に肺循環の速やかな改善を目指して使用する。出血のリスクを評価すべきで，わが国で本症に保険適用があるのはモンテプラーゼだけである。

2）長期治療

ワルファリンをヘパリン投与中から1日3〜5 mgで併用し，INR 2前後(1.5〜2.5)を目標に調整する。投与期間は発症素因により異なるが，3カ月以上投与することが勧められており，がん患者やDVTの再発例ではさらに長期間投与が推奨されている。わが国での知見は十分ではないが，欧米のエビデンスではワルファリンより低分子ヘパリンが推奨されている[4,5,7]。

3）カテーテル治療

カテーテルによる血栓破砕(fragmentation)と血栓吸引(aspiration thrombectomy)が主体で，単にカテーテルを肺動脈に誘導し血栓溶解薬を局所投与する方法の効果は否定的であるがしばしば併用される。血栓吸引にはpercutaneous transluminal coronary angioplasty(PTCA)用ガイディングカテーテルが用いられ，ピッグテイルカテーテルなどで肺動脈内の血栓を破砕し末梢離散させ，その破砕離散した血栓を吸引する方法で，良好な成果の報告がある。

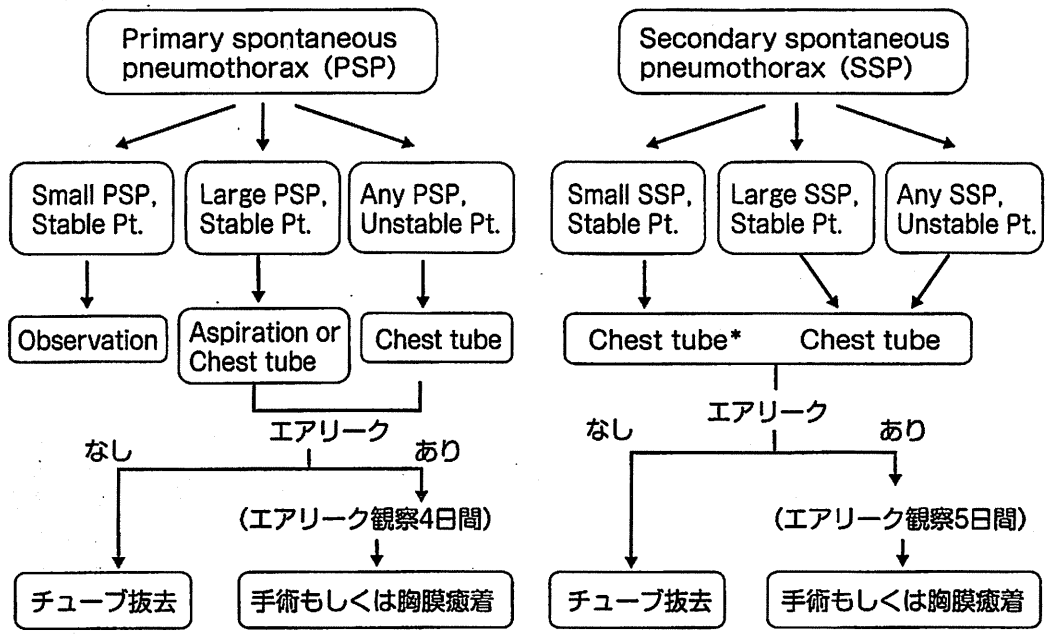

図2 気胸治療アルゴリズム

*注意深い経過観察も許容される。

4）体外循環と外科的治療法

循環不全やショックを呈するような肺動脈幹あるいは両側肺動脈を閉塞するような広範性PEでは，発症時から循環動態が不安定で心停止をきたしたり循環サポートが必要になる。薬剤の治療効果が乏しい症例や血栓溶解療法の適応できないような症例では，施設の整備体制にもよるが，体外循環下に肺動脈血栓摘除術が行われる。

5）下大静脈(IVC)フィルター

PEの直接的治療効果はないがPE再発予防法として，凝固療法が不適当なPEや，不安定な深部静脈血栓症を有したり血栓溶解療法を行う症例，心肺機能の予備力が少ないPE症例に適応することが多い。下大静脈フィルターには永久留置型のものと数週間のうちであれば回収できる非永久留置型のものがある。がん治療の根治的治療時のリスク軽減のために一時的に非永久留置型フィルターを留置することもある。

予後と経過

PEの多くは予防可能であるが，一度発症するとその症状は重篤で急速に致命的となり得る疾患である。わが国でのPEの死亡率は20～30%の報告があり[8,9]，特にショックを呈した症例ほど死亡率が高い(表2)。しかし，早期診断・治療をすることで救命は可能で，急性期を乗り切り予後は比較的良好である。特に担がん患者では手術症例のみならず内科的治療例でも本症の発症リスクが高いことを認識し予防策を講じ，経過中はPEも起こり得ることを考慮した診療が行われるべきと考える。

気胸

気胸の治療に関しては，各医師や医療機関の経験を中心とした治療が行われているのが現状で，その治療法は無作為化比較試験もほとんどなく，科学的に検証された知見が少ないのが現状で[10]，

わが国での気胸治療のガイドラインも完成に至っていない。

気胸の原因・分類・症状は成書に委ねるが，治療方法は患者背景により若干異なる。

1 治 療

気胸の程度，すなわち肺の虚脱レベルや緊張性気胸かどうか，血気胸の有無など患者の状態(stableとunstableに分類)で治療法を細分化している(**図2**)。気胸の初期治療として，虚脱した肺を再膨張させるために安静，脱気，胸腔ドレナージの方法があり，血気胸や緊張性気胸など，気胸により状態が不安定となっていると考えられる場合は迅速な処置が求められることはいうまでもない。

ACCPガイドライン[10]では，ドレナージチューブの種類やサイズ，吸引をするかウォーターシールとするかについてもコメントされているが，エキスパートの意見を集約したものがほとんどで，前述のごとく科学的に検証されたレベルのものはない。4〜5日程度のドレナージ期間で気漏の改善傾向が乏しい場合は，手術あるいは胸膜癒着法を検討すべきである。手術法は胸腔鏡手術，開胸手術があり，患者背景も考慮して検討されるべきで，特に担がん患者では患者への身体的侵襲の少ない手技が求められる。胸膜癒着法ではドキシサイクリン，タルク，ミノサイクリンを推奨しているが，わが国では保険適用がなく，またタルクは入手困難であり，実臨床ではドキシサクリンは製造中止となったためミノサイクリンとピシバニールがよく用いられている。近年，難治性の気胸に対して経気道的塞栓術が有効であるとの報告もみられる。

文 献

1) Khorana AA, Francis CW, Culakova E : Thromboembolism is a leading cause of death in cancer patients receiving outpatient chemotherapy. J Thromb Haemost **5** : 632-634, 2007
2) Ahibrecht J, Dickmann B, Ay C : Tumor grade is associated with venous thrombolism in patients with cancer : Results from the Vienna cancer and thrombosis study. J Clin Oncol **30** : 3870-3875, 2012
3) 肺血栓塞栓症および深部静脈血栓症の診断，治療，予防に関するガイドライン(2009年改訂版)2008年度合同研究班報告
www.j-circ.or.jp/guideline/pdf/JCS2009
4) Noble SI, Shelly MD, Coles B : Management of venous thromboembolism in patients with advanced cancer : a systematic review and meta-analysis. Lancet Oncol **9** : 577-584, 2008
5) Guyatt GH, Akl EA, Crowther M : Antithrombotic therapy and prevention of thrombosis, 9th ED : ACCP Guidelines. Chest **141**(Suppl) : 7S-47S, 2012
6) 肺血栓塞栓症／深部静脈血栓症(静脈血栓塞栓症)予防ガイドライン作成員会：肺血栓塞栓症／深部静脈血栓症(静脈血栓塞栓症)予防ガイドライン，メディカルフロント インターナショナル リミテッド，東京，2004，pp1-96
7) Lyman GH, Khorana AA, Falanga A : American Society of Clinical Oncology Guideline : Recommendations for venous thromboembolism prophylaxis and treatment in patients with cancer. J Clin Oncol **25** : 5490-5505, 2007
8) Chew HK, Wun T, Harvey D : Incidence of venous thromboembolism and its effect on survival among patients with common cancers. Arch Intern Med **166** : 458-464, 2006
9) Ota M, Nakamura M, Yamada N : Prognostic significance of early diagnosis in acute pulmonary thromboembolism with circulatory failure. Heart Vessels **17** : 7-11, 2002
10) Bumann MH, Strange C, Heffner JE : Management of spontaneous pneumothorax : an American College of Chest Physicians Delphi consensus statement. Chest **119** : 590-602, 2001

Ann Nucl Med (2013) 27:781–785
DOI 10.1007/s12149-013-0738-0

CASE REPORT

Oncocytic carcinoid tumor of the lung with intense F-18 fluorodeoxyglucose (FDG) uptake in positron emission tomography–computed tomography (PET/CT)

Yuki Tanabe · Yoshifumi Sugawara · Rieko Nishimura · Kohei Hosokawa · Makoto Kajihara · Teruhiko Shimizu · Tadaaki Takahashi · Shinya Sakai · Shigeki Sawada · Motohiro Yamashita · Haruhiko Ohtani

Received: 7 March 2013 / Accepted: 10 May 2013 / Published online: 12 June 2013

Abstract The present report describes a case of typical carcinoid tumor with intense fluorodeoxyglucose (FDG) uptake. The most of tumor cells were characterized by eosinophilic cytoplasm resulting from accumulation of mitochondria, which was called an oncocytic carcinoid tumor. Glucose transporter type 1 (GLUT-1) was expressed in a membranous pattern in the oncocytic component. Oncocytic carcinoid tumors could show intense FDG uptake due to the numerous intracellular mitochondria and the membranous overexpression of GLUT-1. Thus, it could be a potential pitfall of interpreting FDG-PET/CT image.

Keywords Oncocytic carcinoid tumor · FDG · PET/CT · GLUT-1 · Mitochondria

Introduction

Pulmonary neuroendocrine tumors (NETs) consist of typical carcinoid, atypical carcinoid, large cell neuroendocrine carcinoma (LCNEC) and small cell lung carcinoma (SCLC). Typical carcinoid is a low-grade malignant tumor and the fluorodeoxyglucose (FDG) uptake is usually lower than that of atypical carcinoid, LCNEC, and SCLC [1–3].

We report a case of typical carcinoid tumor with intense FDG uptake in FDG-PET/CT. The most of the tumor cells were characterized by eosinophilic cytoplasm, indicating that it was an oncocytic carcinoid tumor.

Y. Tanabe (✉) · Y. Sugawara · K. Hosokawa · M. Kajihara · T. Shimizu · T. Takahashi · S. Sakai
Department of Diagnostic Radiology, National Hospital Organization, Shikoku Cancer Center, Kou-160 Minamiumemoto-machi, Matsuyama, Ehime 791-0280, Japan
e-mail: yuki.tanabe.0225@gmail.com

R. Nishimura
Department of Clinical Laboratory, National Hospital Organization, Shikoku Cancer Center, Matsuyama, Ehime, Japan

S. Sawada · M. Yamashita
Department of Thoracic Surgery, National Hospital Organization, Shikoku Cancer Center, Matsuyama, Ehime, Japan

H. Ohtani
Department of Radiology, Saiseikai Saijo Hospital, Saijo, Ehime, Japan

Case report

A 68-year-old man had a left lung mass identified by chest X-ray examination 4 years prior. FDG-PET/CT imaging at that time showed a 4-cm round mass with intense FDG uptake in the left lower lobe of the lungs. The FDG-PET/CT scan was performed 1 and 2 h after injection of FDG (185 MBq). The maximum standardized uptake value (SUVmax) of the tumor at 1 h was 38.5 (liver 3.8, mediastinum 2.5) and the SUVmax of the tumor at 2 h was 43.2 (Fig. 1a–c). He underwent bronchoscopic biopsy; however, the histological diagnosis was unevaluable for a little material. Although he was advised to receive surgical treatments, he refused surgery without any symptoms and selected closed follow-up, because of no symptom. Follow-up CT imaging was performed every about 3 months. The tumor was growing gradually.

Four years later, the patient presented with fever, cough, and sputum. Repeat CT revealed enlargement of the left lower mass within the bronchi, accompanied by obstructive pneumonitis. FDG-PET/CT showed increased FDG uptake. The SUVmax of the tumor at 1 h was 45.7 (liver 3.0, mediastinum 2.7) and the SUVmax of the tumor at 2 h was 60.1 (Fig. 1d–f).

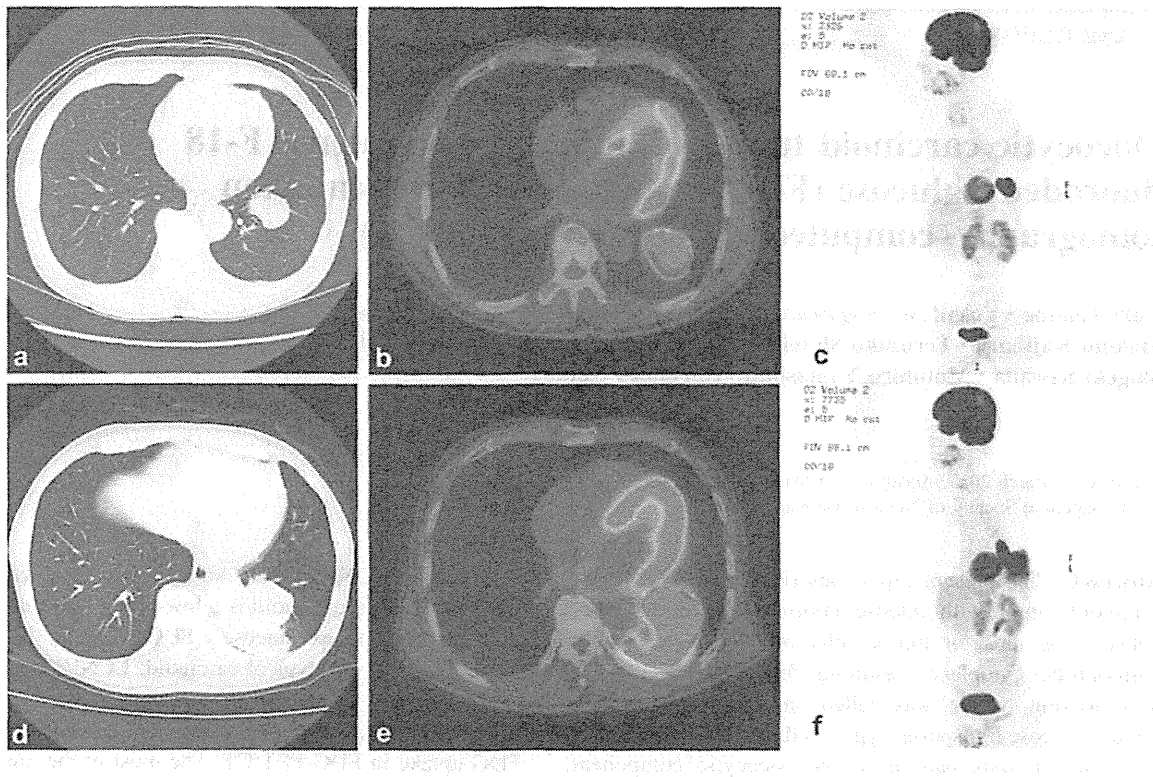

Fig. 1 **a**, **b**, **c** CT image showed mass lesion in the left lower lobe of the lung 4 years ago. FDG-PET/CT images (1 h) showed intense FDG uptake in the mass (SUVmax 38.5) (fusion image in **b**, maximum intensity projection image in **c**). **d**–**f** CT images showed the mass increasing in size, accompanied by obstructive pneumonitis. The FDG uptake (1 h) of the tumor increases (SUVmax 45.7) (fusion image in **e**, maximum intensity projection image in **f**)

There was a discrepancy between the clinical slow progression and intense FDG uptake. Tumor markers [e.g., neuron-specific enolase (NSE), squamous cell carcinoma antigen (SCC), carcinoembryonic antigen (CEA), cytokeratin fragment (CYFRA)] were within normal levels. Bronchoscopic biopsy was performed again, and histological examination revealed a diagnosis of pulmonary carcinoid tumor. He subsequently underwent left lower lobectomy.

Gross examination revealed a 6.0 × 4.5 × 3.0 cm solid tumor arising from the bronchial wall, involving the surrounding lung parenchyma, and occluding the left lower bronchus. The cut surface of the resected specimen appeared largely brown (Fig. 2a filled square) and partially white (Fig. 2a filled circle). Histopathologic examination revealed bland polygonal or spindled cells with scant cytoplasm and finely granular chromatin arranged in organoid nests, trabeculae, or cords characterized tumors (Fig. 2b). The tumor cells were positive for chromogranin A (Fig. 2c), synaptophysin, and CD56. There was no necrosis, and the mitotic rate was low [less than 1 mitosis per 10 high-power field (HPF)]. The ratio of MIB-1 (Ki-67) immunohistochemical staining was less than 5 %. Histological findings were compatible with a typical carcinoid tumor. Moreover, as opposed to the ordinary carcinoid tumors, the majority of the tumor cells had abundant eosinophilic cytoplasm (Fig. 2b filled square). These tumor cells were stained positive for anti-mitochondrial antibody (Fig. 2d filled square). Thus, the tumor was diagnosed as a typical carcinoid tumor of the lung with extensive oncocytic component, i.e., an oncocytic carcinoid tumor. The pathological stage was pStageIIA (pT2b, N0, M0 UICC 7th). The patient has been doing well 1 year after the surgery without local recurrence and metastasis.

Discussion

Pulmonary carcinoid tumors are low-grade NETs and comprise approximately 1–2 % of all lung neoplasms. Previous studies showed that the majority of pulmonary carcinoid tumors arise within the central airways as endbronchial masses [4]. Symptoms associated with pulmonary carcinoid tumors are due to bronchial obstruction and include cough, shortness of breath, wheezing, and hemoptysis. Recent reports describe peripheral pulmonary

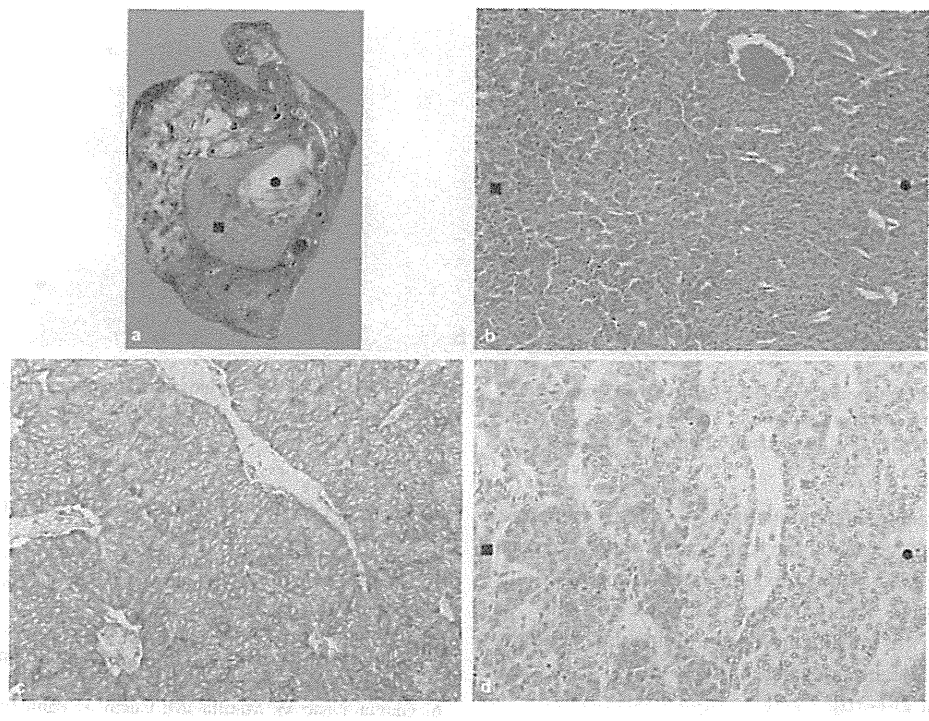

Fig. 2 **a** The cut surface of the tumor appears largely *brown (filled square)* and partially *white (filled circle)*. **b** HE staining sections show bland polygonal or spindled cells arranged in organoid nests, trabeculae, or cords. The tumor cells on the left side have eosinophilic cytoplasm (*reddish colored filled square*). This area is the oncocytic component. **c** The tumor cells are positive for chromogranin A (*brown colored*). **d** The tumor cells with eosinophilic cytoplasm are positive for anti-mitochondrial antibody (*brown colored filled square*)

carcinoid tumors detected incidentally as solitary pulmonary nodules in asymptomatic patients [5]. Pulmonary carcinoid tumors can be categorized as typical and atypical carcinoid tumors on the basis of histological criteria. Typical carcinoid tumors contain less than two mitoses per ten HPF without necrosis. Atypical carcinoid tumors contain increased mitoses (2–10 mitoses per HPF) or necrosis. Atypical carcinoid tumors are more aggressive, with a higher incidence of vascular invasion, metastases, and recurrence. The 5-year survival rate of atypical carcinoid tumors (68–78 %) is lower than that of typical carcinoid tumors (93–98 %) [6, 7].

Oncocytic carcinoid tumors are a rare variant of pulmonary carcinoid tumors. The distinctive feature is the predominant oncocytic component, which consists of tumor cells with eosinophilic cytoplasm resulting from accumulation of mitochondria. Oncocytic change might be the result of mitochondrial dysfunction and associated defects in cellular metabolism [8]. However, the tumorigenesis of oncocytic change remains controversial. Tsuta et al. [9] described 15 cases of oncocytic carcinoid tumors of the lung and reported that there was no appreciable difference between oncocytic carcinoid tumors and non-oncocytic carcinoid tumors in terms of clinical features, age, pathological stage, and 5-year recurrence-free survival. However, the number of cases in this study was small, and examination of additional cases if needed to fully delineate the clinical features of oncocytic carcinoid tumors.

In FDG-PET/CT images, typical carcinoid tumors usually show lower FDG uptake than LCNEC and SCLC because of their hypometabolic activity [1–3]. In the present case, however, FDG-PET/CT imaging showed very intense FDG uptake (SUVmax 60.1), which is contrary to that seen for the typical carcinoid tumor with low proliferative activity. Similarly, some investigators have observed high FDG uptake in typical carcinoid tumors with oncocytic component [10, 11]. These tumors commonly have eosinophilic cells, which are the result of mitochondrial hyperplasia. Thus, these cells might be the cause of FDG uptake in these benign or low-grade malignant tumors, and the existence of rich mitochondria might be directly or indirectly associated with this phenomenon.

Uptake of FDG is based on the increased glucose metabolism of malignant cells [12, 13]. FDG, a glucose analog, enters tumor cells via glucose transporters (GLUT) which are transmembrane proteins that mediate cellular glucose uptake. Glucose transporter type 1 (GLUT-1) is the main subtype of GLUT that determines FDG uptake in tumor cells [12]. We examined the expression of GLUT-1

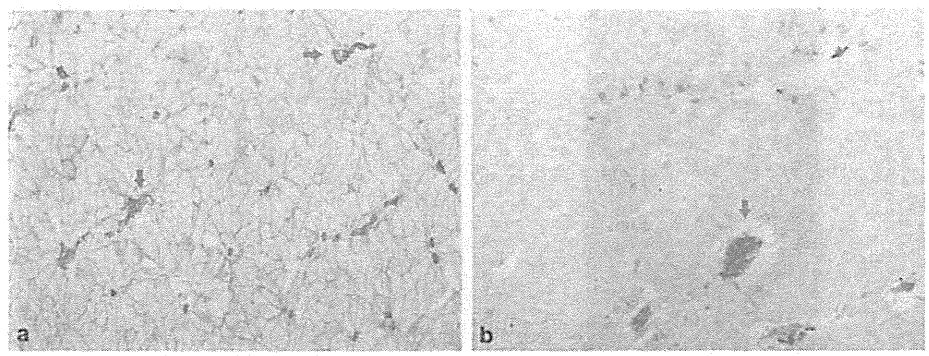

Fig. 3 **a** In the oncocytic component, GLUT-1 is overexpressed in membranous pattern (*brown reticulate stained*). Red cells are naturally stained for GLUT-1 (*red arrow*). **b** In the non-oncocytic component, GLUT-1 is less expressed than the oncocytic component. Red cells are also stained for GLUT-1 (*red arrow*)

in the resected specimen. Interestingly, GLUT-1 was more overexpressed in the oncocytic component than the non-oncocytic component. Moreover, the expression was along the cell membrane (membranous pattern) (Fig. 3a, b). Since GLUT-1 is a transmembrane protein, the membranous pattern should be considered when GLUT-1 expression is evaluated [14–16].

The present case suggested that GLUT-1 membranous expression in the oncocytic component might account for the high FDG uptake in this typical carcinoid tumor. In the pulmonary NET, the GLUT-1 expression and FDG uptake of the tumor increase proportionally as the tumor becomes more malignant [16, 17]. However, we assumed that the intense FDG uptake in this case was not related to the cell proliferation due to the slow growing course and no metastasis in lymph nodes and other organs. For limitations, we could not examine the other important factors for FDG uptake, such as hexokinase activity.

We reported an interesting case of oncocytic carcinoid tumors with intense FDG uptake and suggested that it could be a potential pitfall of interpreting FDG-PET/CT image. Actually, in most clinical cases, such tumors with intense FDG uptake should be excised because it is considered to be malignant tumors.

Acknowledgments We thank Dr. Tomoko Wakasa and Dr. Masayuki Shintaku of Osaka Red Cross Hospital and Professor Yukio Takeshima of Hiroshima University Graduate School of Medicine for immunohistochemical stainings.

References

1. Erasmus JJ, McAdams HP, Patz EF Jr, Coleman RE, Ahuja V, Goodman PC. Evaluation carcinoid of primary pulmonary tumors using FDG PET. AJR. 1998;170:1369–73.
2. Kruger S, Buck AK, Blumstein NM, Pauls S, Schelzig H, Kropf C, et al. Use of integrated FDG PET/CT imaging in pulmonary carcinoid tumours. J Intern Med. 2006;260:545–50.
3. Chong S, Lee KS, Kim BT, Choi JY, Yi CA, Chung MJ, et al. Integrated PET/CT of pulmonary neuroendocrine tumors: diagnostic and prognostic implications. AJR. 2007;188:1223–31.
4. Modlin IM, Lye KD, Kidd M. A 5-decade analysis of 13,715 carcinoid tumors. Cancer. 2003;97:934–59.
5. Meisinger QC, Klein JS, Butnor KJ, Gentchos G, Leavitt BJ. CT features of peripheral pulmonary carcinoid tumors. AJR. 2011; 197:1073–80.
6. García-Yuste M, Matilla JM, Cueto A, Paniagua JM, Ramos G, Canizares MA, et al. Typical and atypical carcinoid tumours: analysis of the experience of the Spanish multi-centric study of neuroendocrine tumours of the lung. Eur J Cardiothorac Surg. 2007;31:192–7.
7. Soga J, Yakuwa Y. Bronchopulmonary carcinoids: an analysis of 1,875 reported cases with special reference to a comparison between typical carcinoids and atypical varieties. Ann Thorac Cardiovasc Surg. 1999;5:211–9.
8. Chang A, Harawi SJ. Oncocytes, oncocytosis, and oncocytic tumors. Pathol Annu. 1992;27:263–304.
9. Tsuta K, Kalhor N, Raso MG, Wistuba II, Moran CA. Oncocytic neuroendocrine tumors of the lung: histopathologic spectrum and immunohistochemical analysis of 15 cases. Hum Pathol. 2011;42: 578–85.
10. Kadowaki T, Yano S, Araki K, Tokushima T, Morioka N. A case of pulmonary typical carcinoid with an extensive oncocytic component showing intense uptake of FDG. Thorax. 2011;66: 361–2.
11. Turan O, Ozdogan O, Gurel D, Onen A, Kargi A, Sevinc C. Growth of a solitary pulmonary nodule after 6 years diagnosed as oncocytic carcinoid tumour with a high 18-fluorodeoxyglucose (18F-FDG) uptake in positron emission tomography–computed tomography (PET-CT). Clin Respir J. 2012;7:e1–5.
12. Mamede M, Higashi T, Kitaichi M, Ishizu K, Ishimori T, Nakamoto Y, et al. [18F] FDG uptake and PCNA, Glut-1, and Hexokinase-II expressions in cancers and inflammatory lesions of the lung. Neoplasia. 2005;7:369–79.
13. Khandani AH, Whitney KD, Keller SM, Isasi CR. Donald Blaufox M. Sensitivity of FDG PET, GLUT1 expression and proliferative index in bronchioloalveolar lung cancer. Nucl Med Commun. 2007;28:173–7.
14. Kalir T, Wang BY, Goldfischer M, Haber RS, Reder I, Demopoulos R, et al. Immunohistochemical staining of GLUT1 in benign, borderline, and malignant ovarian epithelia. Cancer. 2002;94:1078–82.
15. Chung JH, Cho KJ, Lee SS, Baek HJ, Park JH, Cheon GJ, et al. Overexpression of Glut1 in lymphoid follicles correlates with

false-positive (18)F-FDG PET results in lung cancer staging. J Nucl Med. 2004;45:999–1003.
16. Lee HJ, Yoo SB, Lee WW, Chung DH, Seo JW, Chung JH. Differential expression of Glut1 in pulmonary neuroendocrine tumors: correlation with histological grade. Korean J Pathol. 2009;43:201–5.
17. Song YS, Lee WW, Chung JH, Park SY, Kim YK, Kim SE. Correlation between FDG uptake and glucose transporter type 1 expression in neuroendocrine tumors of the lung. Lung Cancer. 2008;61:54–60.

CHEST

Original Research

LUNG CANCER

Risk Factors for Recurrence After Lung Cancer Resection as Estimated Using the Survival Tree Method

Shigeki Sawada, MD, PhD; Natsumi Yamashita, MD, PhD; Hiroshi Suehisa, MD, PhD; and Motohiro Yamashita, MD, PhD

Background: **Patients with lung cancer often present with recurrence, even after resection. The identification of risk factors for recurrence after resection is useful.**
Methods: **Among 1,338 patients with lung cancer who underwent a complete resection, 277 developed recurrences post surgery. Data regarding the TNM factors, histologic subtype, and presence/absence of vessel invasion were analyzed retrospectively using the survival tree method to identify groups with a high risk of recurrence after resection.**
Results: **The results revealed that the T factor, the N factor, and lymphatic (ly) and blood (v) vessel invasion were related to the risk of recurrence, and six combinations of these factors were identified using the survival tree method: group A: v = 0, T ≤ 1b, ly = 0; group B: v = 0, T ≤ 1b, ly ≥ 1; group C: v = 0, T ≥ 2a; group D: v ≥ 1, N ≤ 1, T ≤ 2b; group E: v ≥ 1, N ≤ 1, T ≥ 3; and group F: v ≥ 1, N ≥ 2. The six groups were then further classified into three groups: a low-risk group (group A), a moderate-risk group (groups B, C, and D), and a high-risk group (groups E and F). The 5-year recurrence-free survival rate was approximately 98% for the low-risk group, 75% for the moderate-risk group, and 30% for the high-risk group.**
Conclusions: **Combining the T, N, v, and ly factors allowed the precise identification of a group with a high risk of recurrence after resection.** ***CHEST 2013; 144(4):1238–1244***

Abbreviations: G = tumor differentiation grade; ly = lymphatic vessel invasion; NSCLC = non-small cell lung cancer; p = pathologic; RFS = recurrence-free survival; v = blood vessel invasion

The TNM staging system for non-small cell lung cancer (NSCLC) is an internationally accepted system used to determine the disease stage.[1-3] This staging system is a measure of the extent of disease and is used to guide management and predict patient prognosis.[4] Surgical resection is performed in patients with stage I and stage II disease as well as in some patients with stage IIIA disease. Examinations, including physical examinations, chest radiography, and so forth, are performed periodically after resection, in accordance with a generally recognized postoperative follow-up or surveillance protocol. The purpose of postoperative follow-up is to detect any recurrences early after resection, so that adequate treatment can be offered in an attempt to improve the survival duration and quality of life. For doctors in charge of such postoperative follow-up, it would be useful to have an understanding of the factors associated with a high risk of recurrence and of the interval until the development of recurrence after resection. The TNM stage is well known to be associated with prognosis. Other factors, such as the presence/absence of vessel invasion and the tumor differentiation grade (G), have also been reported to be associated with prognosis.[5-7] In this study, to identify a population with a high risk of recurrence after resection for NSCLC, we evaluated the T factor, N factor, extent of vessel invasion, and so on as part of

Manuscript received December 19, 2012; revision accepted April 19, 2013.
Affiliations: From the Department of Thoracic Surgery (Drs Sawada, Suehisa, and M. Yamashita), and the Division of Clinical Biostatistics (Dr N. Yamashita), National Hospital Organization Shikoku Cancer Center, Matsuyama, Japan.
Funding/Support: The authors have reported to *CHEST* that no funding was received for this study.
Correspondence to: Shigeki Sawada, MD, PhD, Department of Thoracic Surgery, Shikoku Cancer Center, 160 Minamiumemoto-cho Kou, Matsuyama-shi, Ehime, 791-0280, Japan; e-mail: ssawada@shikoku-cc.go.jp

DOI: 10.1378/chest.12-3034